frontiers
in Earth Science

CORRECTION
published: 03 August 2021
doi: 10.3389/feart.2021.723763

Corrigendum: Magmatic Processes at La Soufrière de Guadeloupe: Insights From Crystal Studies and Diffusion Timescales for Eruption Onset

Abigail Metcalfe[1]*, *Séverine Moune*[1,2,3], *Jean-Christophe Komorowski*[1], *Geoff Kilgour*[4], *David E. Jessop*[1,2,3], *Roberto Moretti*[1,2] *and Yoann Legendre*[5]

[1]Institut de Physique du Globe de Paris, CNRS, Université de Paris, Paris, France, [2]Observatoire Volcanologique et Sismologique de Guadeloupe, Institut de Physique du Globe de Paris, Gourbeyre, France, [3]CNRS, IRD, OPGC Laboratoire Magmas et Volcans, Université Clermont Auvergne, Clermont-Ferrand, France, [4]Wairakei Research Centre, GNS Science, Taupō, New Zealand, [5]Bureau de Recherches Géologiques et Minières, Guadeloupe, France

Keywords: diffusion timescales, orthopyroxene, magma "mush", unrest, monitoring, eruption style, forecasting, La Soufrière de Guadeloupe

A Corrigendum on

Magmatic Processes at La Soufrière de Guadeloupe: Insights From Crystal Studies and Diffusion Timescales for Eruption Onset
by Metcalfe, A., Moune, S., Komorowski, J.-C., Kilgour, G., Jessop, D. E., Moretti, R., and Legendre, Y. (2021). Front. Earth Sci. 9:617294. doi:10.3389/feart.2021.617294

OPEN ACCESS

Edited and reviewed by:
Fabio Arzilli,
The University of Manchester,
United Kingdom

****Correspondence:***
Abigail Metcalfe
metcalfe@ipgp.fr

Specialty section:
This article was submitted to Volcanology,
a section of the journal
Frontiers in Earth Science

Received: *11 June 2021*
Accepted: *21 July 2021*
Published: *03 August 2021*

Citation:
Metcalfe A, Moune S, Komorowski J-C, Kilgour G, Jessop DE, Moretti R and Legendre Y (2021) Corrigendum: Magmatic Processes at La Soufrière de Guadeloupe: Insights From Crystal Studies and Diffusion Timescales for Eruption Onset.
Front. Earth Sci. 9:723763.
doi: 10.3389/feart.2021.723763

In the original article, there was a mistake in **Table 2** and in **Figures 5**, **9** and **10** as published. An error occurred in our calculations of the D_0 value, which was then propagated into the numerical routines used to perform our calculations. Calculations with the corrected D_0 value imply that the timescales of magmatic processes preceding eruptions of La Soufrière de Guadeloupe, shown in **Table 2**, and discussed in our original manuscript, are lower than previously estimated by a factor of ~2. The corrected **Table 2** and **Figures 5** and **9** appear below. The corrected **Figure 10** also appears below, and the trend of the figure is not altered.

Further errors were made in **Figures 11**, **12** and **13**. The timescales are now corrected in the captions of the figures. The correct timescale values, now presented below, range from 18.8 to 361.0 days confirming that magmatic processes prior to eruption occur on short timescales at La Soufrière de Guadeloupe. Updated and corrected versions of our python scripts are available on GitHub: https://github.com/djessop/mineral_diffusion_timescales. The corrected figures appear below.

A correction has been made to the **Abstract**, Paragraph 3:

"We model the timescale populations as random processes whose probability distributions provide expected ("mean") timescales and the associated standard errors for each eruption. This provides a new statistical method for comparing magmatic timescales between disparate eruptions. From this, we obtain timescales of magma storage at La Soufrière de Guadeloupe ranging from 18.8 ± 0.37 days to 361 ± 0.40 days, with no clear distinction between eruption style/size and timescales observed. Based on these data, magmatic interaction timescales are a poor predictor of eruption style/size."

A correction has also been made to Section **Results**, Sub-section **Timescale Modelling Results**, Paragraphs 1–4:

"Diffusion timescales across the core-rim boundaries for the eruptions studied give a timescale range from <1 to 3,052 days (**Table 2**). Our method has investigated how the timescale populations are distributed, highlighting clear differences between eruptions, including variations in the maximum values, range of values and expected timescales.

TABLE 2 | Summary table for the eruptions showing the key features for each eruption and sample location.

Eruption	Vent	Sample GPS position			Eruption style	Expected timescale (days)	Median timescale (days)	Min. timescale (days)	Max. timescale (days)	Timescale std. error (days)	Crystals analysed	Temp °C (±30°C)	Av. Bulk SiO_2 (wt %)	VEI
		UTM N (m)	UTM O (m)	Unit sampled from										
1657 CE	Soufrière	641,466	1,773,774	Fallout Unit	Vulcanian	18.8	12.00	0.1	84.3	0.37	41	975	58.1	2–3
1530 CE	Soufrière	643,318	1,774,407	Fallout Unit	Sub-Plinian	20.5*	—	10	90	—	24	900	57.5	3
1010 CE	Soufrière	638,266 638,228	1,769,743 1,769,738	Fallout Unit	Plinian	361.0	192.2	0.4	2,462.3	0.40	34	1,025	59.7	4
341 CE	Echelle	663,019	178,011	Scoria Clasts	Strombolian	59.4	30.9	0.4	3,051.7	0.40	33	1,010	51.2	2
5680 BCE	Soufrière	637,417	1,770,276	Fallout Unit	Plinian	22.8	11.2	0.9	167.9	0.43	31	1,010	—	4

*The crystal number refers to the number of crystals diffusion timescales were calculated on [*Mean timescale not expected timescale, calculated from available data Bourgeoisat (2018); Boudon et al. (2008); Pichavant et al. (2018)].*

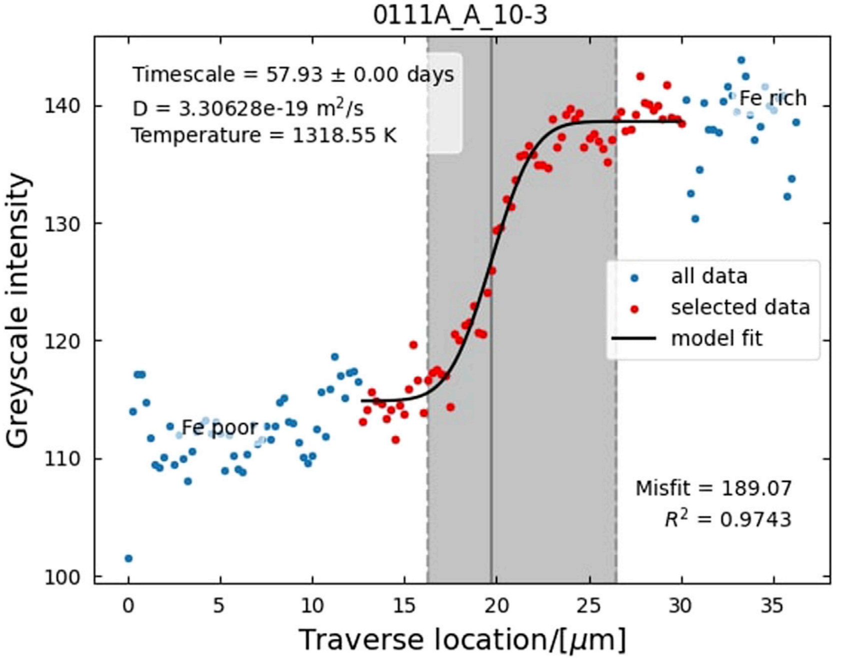

FIGURE 5 | SEM greyscale intensity as a function of traverse location extracted from the SEM image for a sample from the 1010 Cal. CE eruption (blue dots), the data selected for fitting by the model (red dots), and the model solution (black line). Also shown are the fitted parameters (timescale, diffusion coefficient, D, and effective temperature), the theoretical profile midpoint (μ–gray line), and the "goodness-of-fit" (R). The gray shaded area represents the mean ±1 SD of the selected data.

The 5680 Cal. BCE Plinian eruption records short timescales with a range from <1 to 169 days and the expected (mean) timescale calculated as 22.8 ± 0.43 days (**Figure 9**). The ~341 Cal. CE Strombolian eruption records a large range of timescales from <1 to 3,052 days. The modelled data yield an expected timescale value of 59.4 ± 0.40 days. This expected value is not comparable to any other eruption studied, though the range of values is comparable.

The 1010 Cal. CE Plinian eruption records the longest timescales from <1 to 2,462 days. These data have an expected timescale value of 361.0 ± 0.40 days, considerably higher than calculated for any other eruption (**Figure 9**). This eruption is considerably different to the 5680 Cal. BCE Plinian eruption, despite the expectation that these eruptions are comparable. This is a direct consequence of the characteristic crystal populations in the 1010 Cal. CE eruption which shows a large proportion of

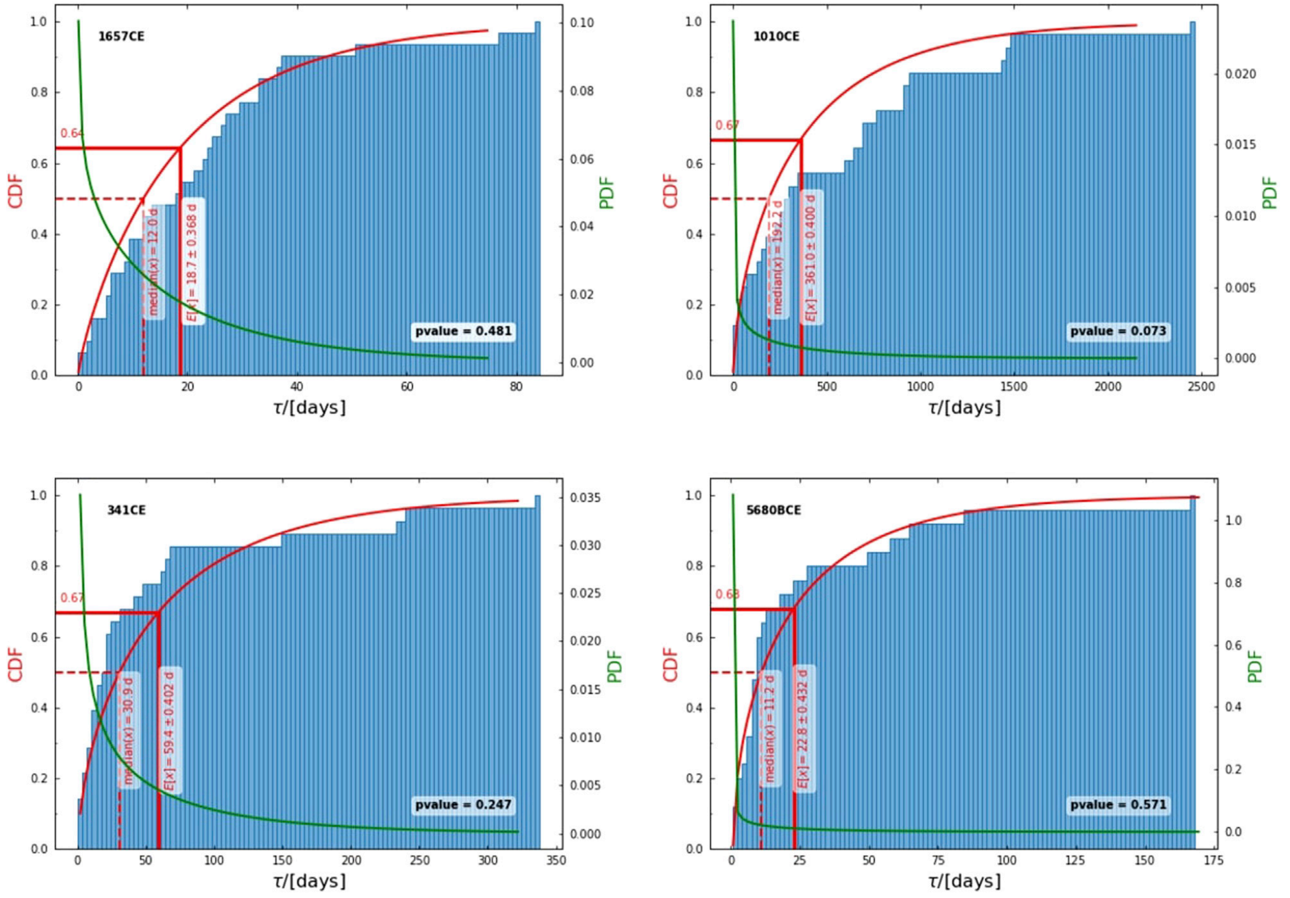

FIGURE 9 | Distribution of timescales for the 1657 Cal. CE, 1010 Cal. CE, ~341 Cal CE and 5680 Cal. BCE eruptions. Blue bars indicate the empirical cumulative density frequencies (CDF), red curves indicate the theoretical distributions fitted to these and the green curves represent the theoretical probability density frequencies. On each plot we indicate the mean and median timescales predicted by the theoretical distributions and the *p*-values (goodness-of-fit) between model and data.

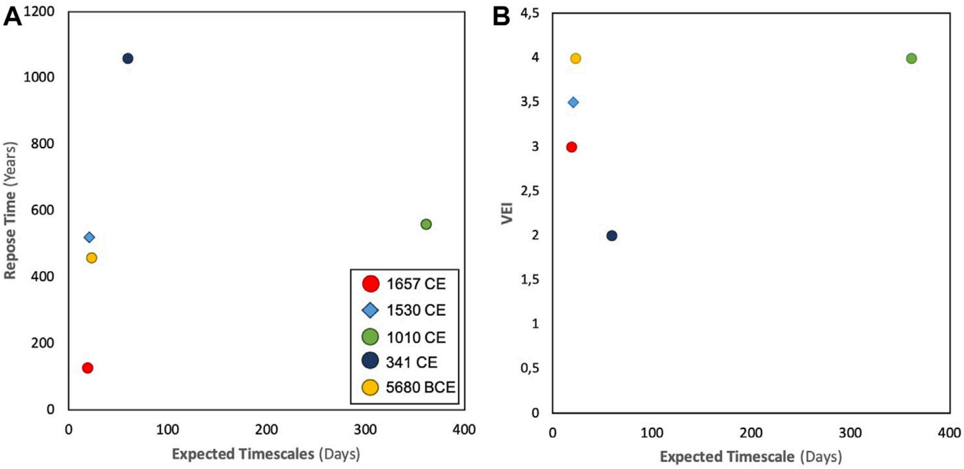

FIGURE 10 | Expected timescale variation diagrams for **(A)** Repose Time, **(B)** Volcanic Explosive Index (VEI). Repose time for the 5680 Cal. BCE eruption is based a collapse event at 7160 Cal. BCE, the closest datable event. *1530 Cal. CE eruption data from Boudon et al. (2008); Bourgeoisat (2018); Pichavant et al. (2018).

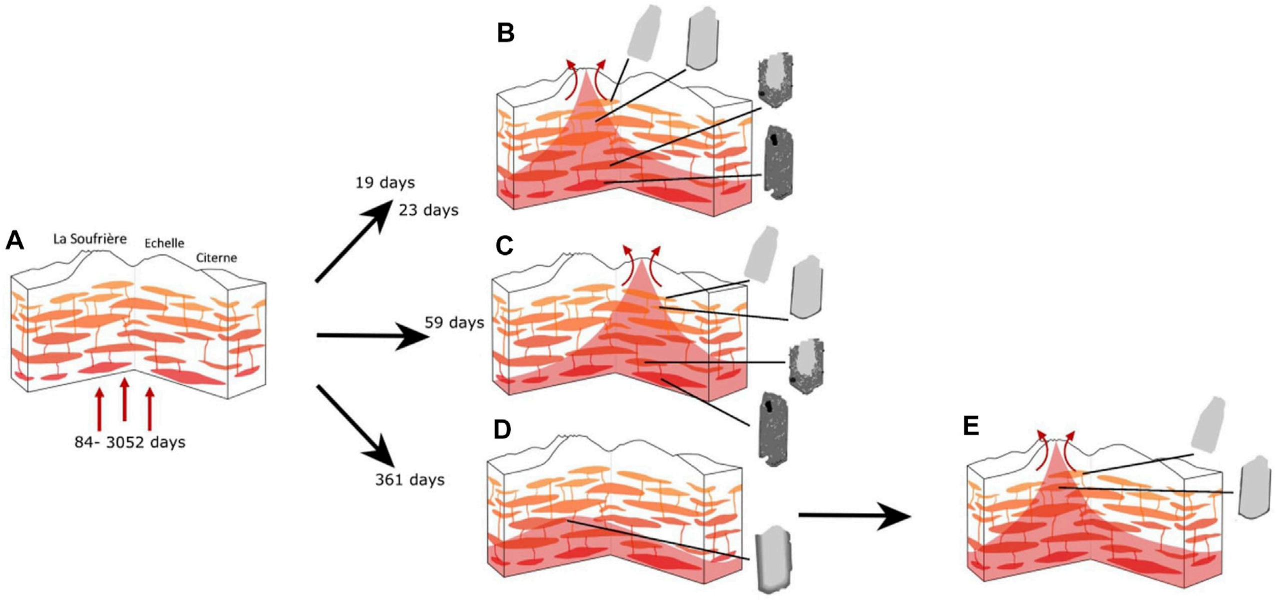

FIGURE 11 | Schematic sketches of the mush lenses beneath La Soufrière de Guadeloupe and Echelle with representative crystals shown at approximate locations within the mush zone. **(A)** The La Soufrière de Guadeloupe mush system prior to eruption, this study suggests intrusions begin a between a minimum of 84 and 3,052 days prior to eruption. **(B)** In the case of 1657 Cal. CE and 5680 Cal. BCE eruptions, the expected value shows that the majority of the system could be affected by an intrusion 19 and 23 days prior to eruption, respectively. The intrusion moves through the system rapidly, in the case of the 5680 Cal. BCE eruption crystals are erupted from deep in the mush system which re-equilibrate during smaller intrusion events which do not destabilise the mush system. The 1657 Cal. CE eruption only samples simple crystals and unzoned crystals. **(C)** The ~341 CE eruption expected value shows that the majority of the system could be affected by an intrusion 59 days before eruption. This intrusion has also moved relatively rapidly through the system and variation in intrusion location, results in destabilisation and eruption from the Echelle vent. Both complex and simple crystal populations are erupted. **(D)** Processes resulting in the 1010 Cal. CE eruption occurred slower than the other eruptions with the expected value showing the majority of the system could be affected by an intrusion 361 days prior to eruption. The very long delay time suggests that magma may have stalled in the mid-upper mush system, crystals with the diffuse zoning have spent the longest time in contact with the intrusion. **(E)** System destabilisation results in eruption of populations of simply zoned and unzoned crystals, perhaps from the upper lenses.

Type-2 crystals with diffuse zoning, not present in the 5680 Cal. BCE eruption (Figure 8).

The 1657 Cal. CE Vulcanian eruption records the shortest range of timescales from <1 to of 84 days. The expected timescale was calculated as 18.8 ± 0.37 days, the shortest expected timescale value calculated for the eruptions studied (**Figure 9**). This expected value is comparable to the 5680 Cal. BCE expected value of 22.8 days, with most crystals for both these eruptions recording timescales in the range of 3 weeks."

A correction has been made to Section **Discussion,** Subsection **How Do We Interpret the Diffusion Timescales**, Paragraph 4:

"These processes are reflected in the gamma distribution, which describes all events that share the same properties (i.e., are generated by the same process) and models them as random processes. In this case, the gamma distribution is derived from the individual likelihood of all intrusion events across the eruption's crystal populations. The timescale distribution reflects an intrusion producing a mixing bowl where the crystals come into contact with the intrusion at different times, with the expected timescale being the typical value of the distribution. The expected timescale/typical distribution value shows the average time it took a crystal for a specific eruption to come into contact with the intrusion. Therefore, the gamma distribution allows the probability of a crystal experiencing an event at a given time to be estimated. In the case of La Soufrière de Guadeloupe, crystals have a smaller probability of recording a short delay time/longer timescale (on the order of a year; e.g., 1010 Cal. CE), and a larger probability of recording a longer delay time/shorter timescale (on the order of days; e.g., 1657 Cal. CE). This could relate to several parameters including: the intrusions interaction with the system, the composition of the system (including volatile content) and system geometry (crystals recording a longer delay time/shorter diffusion timescale farthest from the intrusion are more likely to be erupted than those closer to the system base which interact with the intrusion first)."

A correction has been made to Section **Discussion,** Subsection **Which Mush System Processes are the Timescales Related To?**, Paragraph 5:

"The ~341 Cal. CE and 1010 Cal. BCE eruptions have similar maximum diffusion timescales but different expected timescales (**Table 2**). This indicates while intrusions may begin at similar times prior to an eruption, the diffusion timescale distribution and resulting expected timescales, suggest the intrusions interact differently with the system. A transition in conduit location to Echelle or the eruption of a monogenetic cone may result in different expected timescales of magmatic processes preceding

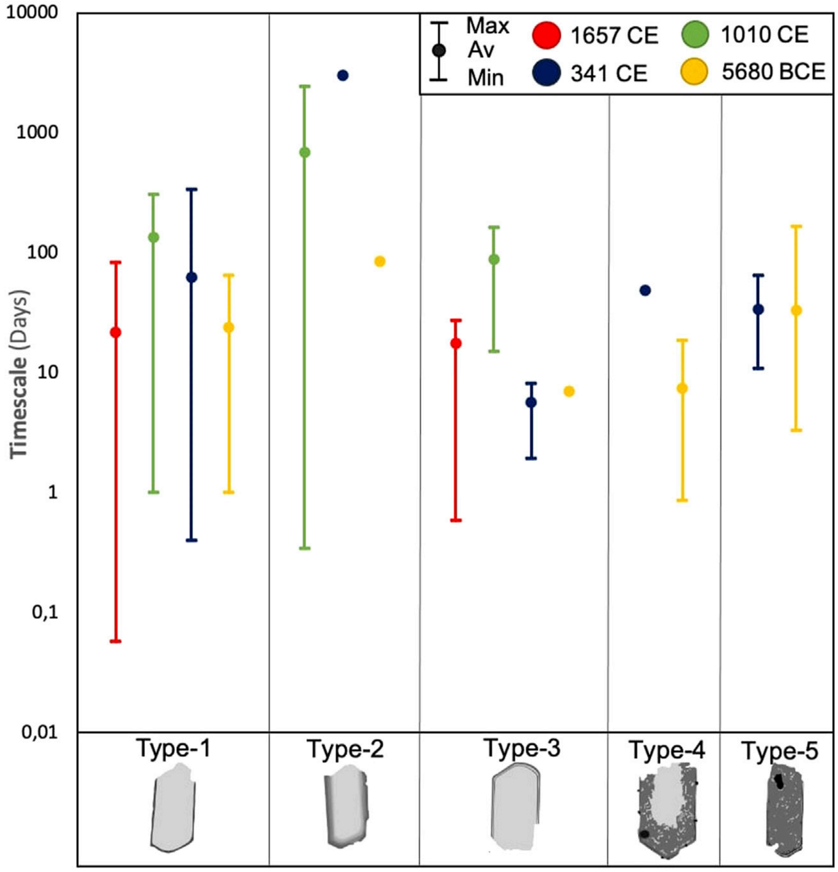

FIGURE 12 | Maximum, minimum and average timescale values for the different crystal populations recorded in each eruption. For single points, only one crystal was identified. The largest range of values are observed in the simple crystals Type-1 and Type-2; however, this may be a reflection of population size. Type-1 is found in all eruptions and records the shortest timescales. Type-2, is mainly found in the 10101 Cal. CE eruption and records the longest timescales and a large range of timescales. Type-3 has the fewest number of crystals and shows the smallest range of values. While the 1657 Cal. CE, ~341 Cal. CE and 5680 Cal. BCE eruptions show similar averages, the 1010 Cal. CE eruption shows a higher average and minimal overlaps with the other eruptions.

eruptions. In a shallow storage region, crystals interact with melt shortly before eruption and could explain the crystals recording short timescales observed, particularly in Echelle and in other monogenetic systems (Ruprecht et al., 2007; Johnson et al., 2008; Denis et al., 2013; Brenna et al., 2018; **Figure 11A,C**)."

A correction has been made to Section **Discussion,** Subsection **How Do the La Soufrière de Guadeloupe Timescales Fit Into a Global Context**, Paragraph 3:

"Some systems show magmatic processes occurring on timescales comparable to La Soufrière de Guadeloupe, such as the 1912 eruption of Novarupta (Alaska), which shows similarly short diffusion timescales. A smaller range of timescales are calculated for this eruption, but the average value, 45 days, is comparable to the expected values calculated for the 1657 Cal. CE, ~341 Cal. CE and 5680 Cal. CE eruptions (Singer et al., 2016). Despite the similarities in the timescales, the Novarupta system is much larger and is more evolved than La Soufrière de Guadeloupe, limiting the comparability."

A correction has been made to Section **Discussion,** Subsection **Can We Link Timescales to Unrest at La Soufrière de Guadeloupe?**, Paragraph 4:

"In the second scenario, long timescales on the order of a year (i.e., 1010 Cal. CE) suggest similar long unrest periods prior to the eruption could be observed. This unrest, recorded over months or years, may show a gradual increase in seismic activity and thermal anomalies, along with geochemical markers of the rising magma batch, peaking in a shallow degassing signature following its emplacement and the thermal (and chemical) exchange with the residing body. Behaviour corresponding to this scenario was observed prior to the May 2008 Bezymianny eruption, characterised by a decrease of CO_2/H_2O, S/HCl, CO_2/S and CO_2/HCl ratios (Lopez et al., 2013; Davydova et a., 2018)."

Finally, a correction has been made to Section **Conclusions**:

"By investigating a range of eruption styles, we provide an in-depth analysis of the diffusion timescales of magmatic processes occurring at La Soufrière de Guadeloupe and provide new insights in the processes occurring in the mush system. The method constitutes a significant advance for the calculation of orthopyroxene diffusion timescales, eradicating biases induced by fitting the profiles by eye, and optimising data quality by using well-tested and robust numerical schemes and "goodness-of-fit" analyses. The six different crystal population distributions, found

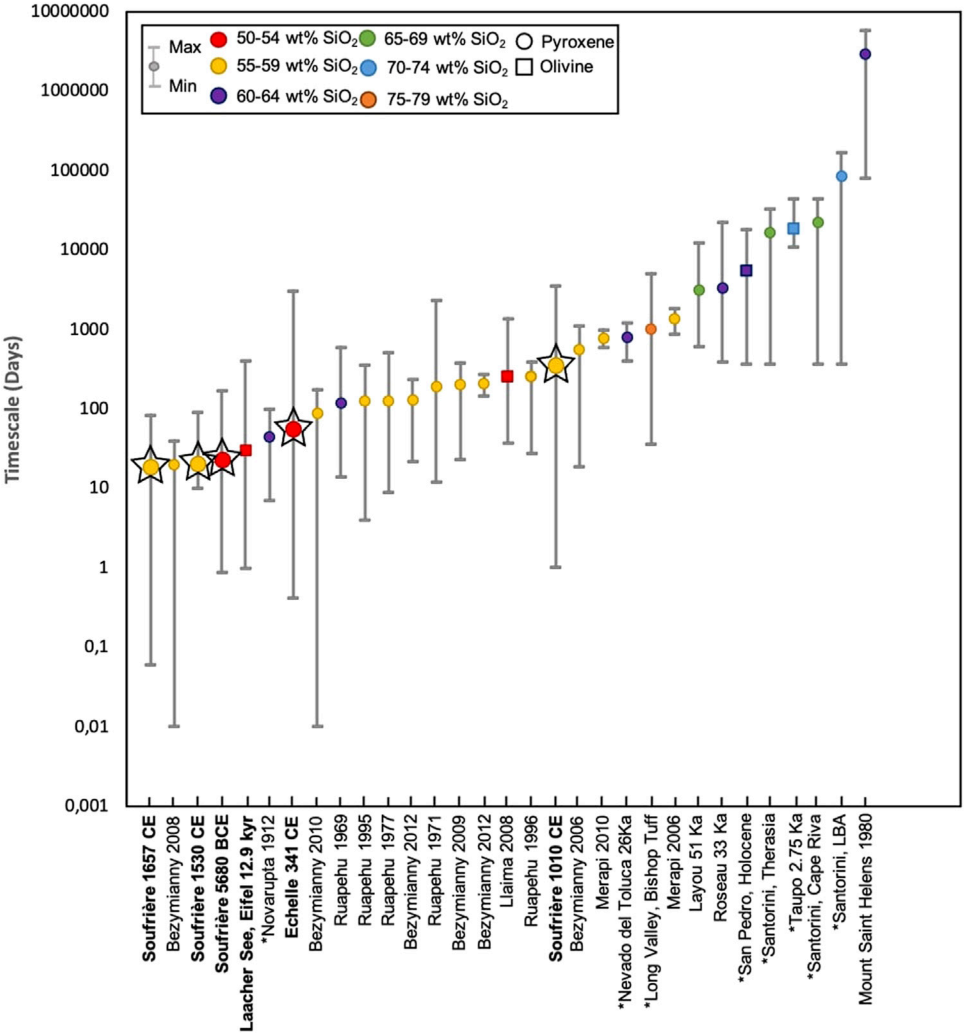

FIGURE 13 | Global database of diffusion timescales (adapted from Costa et al., 2020), for relatively evolved composition eruptions. The majority of studies are done on pyroxene with two examples of olivine studies. This shows the wide range of timescales that can be calculated through diffusion methods, from hours to centuries. Systems incomparable to La Soufrière are marked with an asterisk (*), these systems generally record the longest timescales and are more typically observed in evolved caldera forming systems. The1530 C.E., 1657 Cal. CE and 5680 Cal. BCE (whole rock estimated) eruptions record some of the shortest timescales for systems in a similar compositional range, with timescales most similar to Bezymianny and Novarupta, Alaska, which show similarly short timescales. (Davydova et al., 2018; Boudon et al., 2008; Pichavant et al., 2018; Singer et al., 2016; Ruth et al., 2018; Costa et al., 2013; Weber et al., 2019; Chamberlain et al., 2014; Costa and Chakraborty, 2004; Fabbro et al., 2013; Barker et al., 2016; Flaherty et al., 2018; Kilgour et al., 2014; Gamble et al., 1999; Saunders et al., 2014; Fabbro et al., 2013; Bourgeoisat, 2018; Solaro et al., 2020; Sundermeyer et al., 2020).

across the four various types of eruptions of La Soufrière de Guadeloupe, indicate different eruptions are fed by different mush system lenses, which have distinct histories. We found distinct timescales for similar eruption styles, suggesting the diffusion timescales do not allow us to discriminate between eruptive styles. In detail, we determined expected values of 22.8 ± 0.43 days for the 5680 Cal. BCE Plinian eruption, 59.4 ± 0.40 days for the ~341 Cal. CE Strombolian eruption, 361.0 ± 0.40 days for the 1010 Cal. CE Plinian eruption and 18.8 ± 0.37 days for the 1657 Cal. CE Vulcanian eruption. The 5680 Cal. BCE and 1657 Cal. CE eruption short timescales correlate to short repose suggesting a magma intrusion hotter than the existing mush moved rapidly through the mush system due to the presence of a magma system with a high proportion of melt. The 1010 Cal. CE eruption long-expected timescale and large range of timescales indicates the system remobilised comparatively slowly with new magma interacting with the system slowly. The majority of timescales calculated in this study are short when compared to global data sets calculated for similar systems. This implies basaltic-andesitic to andesitic volcanoes can rapidly produce large-scale eruptions. Paramount for hazard assessment and crisis response, the lack of a correlation between eruption explosive intensity (VEI) and timescales that also applies to short timescales, indicates that a future eruption of La Soufrière de Guadeloupe could broadly span a range from low to high explosivity. These results underscore the necessity to further: improve the reliability of detecting and interpreting multiparameter monitoring data as eruption precursors, expand eruption forecast modelling, develop probabilistic expert judgement for crisis response, as well as enhance risk reduction and societal resilience."

The authors apologize for these errors and state that this does not change the scientific conclusions of the article in any way. The original article has been updated.

REFERENCES

Barker, S. J., Wilson, C. J. N., Morgan, D. J., and Rowland, J. V. (2016). Rapid priming, accumulation, and recharge of magma driving recent eruptions at a hyperactive caldera volcano. *Geology* 44 (4), 323–326. doi:10.1130/g37382.1

Boudon, G., Komorowski, J.-C., Villemant, B., and Semet, M. P. (2008). A new scenario for the last magmatic eruption of La Soufrière of Guadeloupe (Lesser Antilles) in 1530 A.D. Evidence from stratigraphy radiocarbon dating and magmatic evolution of erupted products. *J. Volcanol. Geothermal Res.* 178 (3), 474–490. doi:10.1016/j.jvolgeores.2008.03.006

Bourgeoisat, C. (2018). *Spatio-temporal dynamics of the magmatic reservoir at the origin of the 1530 AD eruption of La Soufrière of Guadeloupe*. Paris: Master's thesis

Brenna, M., Cronin, S. J., Smith, I. E. M., Tollan, P. M. E., Scott, J. M., Prior, D. J., et al. (2018). Olivine xenocryst diffusion reveals rapid monogenetic basaltic magma ascent following complex storage at Pupuke Maar, Auckland Volcanic Field, New Zealand. *Earth Planet. Sci. Lett.* 499, 13–22. doi:10.1016/j.epsl.2018.07.015

Chamberlain, K., Morgan, D., and Wilson, C. (2014). Timescales of mixing and mobilisation in the Bishop Tuff magma body: perspectives from diffusion chronometry. *Contrib. Mineralogy Petrol.* 168 (1). doi:10.1007/s00410-014-1034-2

Costa, F., Andreastuti, S., Bouvet de Maisonneuve, C., and Pallister, J. S. (2013). Petrological insights into the storage conditions, and magmatic processes that yielded the centennial 2010 Merapi explosive eruption. *J. Volcanol. Geothermal Res.* 261, 209–235. doi:10.1016/j.jvolgeores.2012.12.025

Costa, F., and Chakraborty, S. (2004). Decadal time gaps between mafic intrusion and silicic eruption obtained from chemical zoning patterns in olivine. *Earth Planet. Sci. Lett.* 227 (3–4), 517–530. doi:10.1016/j.epsl.2004.08.011

Costa, F., Shea, T., and Ubide, T. (2020). Diffusion chronometry and the timescales of magmatic processes. *Nat. Rev. Earth Environ.* 1 (4), 201–214. doi:10.1038/s43017-020-0038-x

Davydova, V. O., Shcherbakov, V. D., and Plechov, P. Y. (2018). The timescales of magma mixing in the plumbing system of Bezymianny volcano (kamchatka): insights from diffusion chronometry. *Mosc. Univ. Geol. Bull.* 73, 444–450. doi:10.3103/s0145875218050058

Denis, C. M. M., Demouchy, S., and Shaw, C. S. J. (2013). Evidence of dehydration in peridotites from Eifel Volcanic Field and estimates of the rate of magma ascent. *J. Volcanol. Geothermal Res.* 258, 85–99. doi:10.1016/j.jvolgeores.2013.04.010

Fabbro, G., Druitt, T., and Scaillet, S. (2013). Evolution of the crustal magma plumbing system during the build-up to the 22-ka caldera-forming eruption of Santorini (Greece). *Bull. Volcanol.* 75 (12). doi:10.1007/s00445-013-0767-5

Flaherty, T., Druitt, T., Tuffen, H., Higgins, M., Costa, F., and Cadoux, A. (2018). Multiple timescale constraints for high-flux magma chamber assembly prior to the Late Bronze Age eruption of Santorini (Greece). *Contrib. Mineralogy Petrol.* 173 (9). doi:10.1007/s00410-018-1490-1

Johnson, E. R., Wallace, P. J., Cashman, K. V., Granados, H. D., and Kent, A. J. (2008). Magmatic volatile contents and degassing-induced crystallization at Volcán Jorullo, Mexico: implications for melt evolution and the plumbing systems of monogenetic volcanoes. *Earth Planet. Sci. Lett.* 269 (3–4), 478–487. doi:10.1016/j.epsl.2008.03.004

Kilgour, G. N., Saunders, K. E., Blundy, J. D., Cashman, K. V., Scott, B. J., and Miller, C. A. (2014). Timescales of magmatic processes at Ruapehu volcano from diffusion chronometry and their comparison to monitoring data. *J. Volcanol. Geothermal Res.* 288, 62–75. doi:10.1016/j.jvolgeores.2014.09.010

López, T., Ushakov, S., Izbekov, P., Tassi, F., Cahill, C., Neill, O., et al. (2013). Constraints on magma processes, subsurface conditions, and total volatile flux at Bezymianny Volcano in 2007–2010 from direct and remote volcanic gas measurements. *J. Volcanol. Geotherm. Res.* 263, 92–107.

Gamble, J. A., Wood, C. P., Price, R. C., Smith, I. E. M., Stewart, R. B., and Waight, T. (1999). A fifty year perspective of magmatic evolution on Ruapehu Volcano, New Zealand: verification of open system behaviour in an arc volcano. *Earth Planet. Sci. Lett.* 170 (3), 301–314. doi:10.1016/s0012-821x(99)00106-5

Pichavant, M., Poussineau, S., Lesne, P., Solaro, C., and Bourdier, J.-L. (2018). Experimental parametrization of magma mixing: application to the ad 1530 eruption of La Soufrière, Guadeloupe (lesser antilles). *J. Petrol.* 59 (2), 257–282. doi:10.1093/petrology/egy030

Ruth, D., Costa, F., Bouvet de Maisonneuve, C., Franco, L., Cortés, J., and Calder, E. (2018). Crystal and melt inclusion timescales reveal the evolution of magma migration before eruption. *Nat. Commun.* 9 (1). doi:10.1038/s41467-018-05086-8

Saunders, K., Buse, B., Kilburn, M. R., Kearns, S., and Blundy, J. (2014). Nanoscale characterisation of crystal zoning. *Chem. Geology.* 364, 20–32. doi:10.1016/j.chemgeo.2013.11.019

Singer, B. S., Costa, F., Herrin, J. S., Hildreth, W., and Fierstein, J. (2016). The timing of compositionally-zoned magma reservoirs and mafic 'priming' weeks before the 1912 Novarupta-Katmai rhyolite eruption. *Earth Planet. Sci. Lett.* 451, 125–137. doi:10.1016/j.epsl.2016.07.015

Solaro, C., Balcone-Boissard, H., Morgan, D. J., Boudon, G., Martel, C., and Ostorero, L. (2020). A system dynamics approach to understanding the deep magma plumbing system beneath Dominica (Lesser Antilles). *Front. Earth Sci.* 8. doi:10.3389/feart.2020.574032

Sundermeyer, C., Gätjen, J., Weimann, L., and Wörner, G. (2020). Timescales from magma mixing to eruption in alkaline volcanism in the Eifel volcanic fields, western Germany. *Contrib. Mineralogy Petrol.* 175 (8), 1–23. doi:10.1007/s00410-020-01715-y

Weber, G., Arce, J. L., Ulianov, A., and Caricchi, L. (2019). A recurrent magmatic pattern on observable timescales prior to plinian eruptions from nevado de Toluca (Mexico). *J. Geophys. Res. Solid Earth* 124, 10999–11021. doi:10.1029/2019jb017640